

Supporting Information

Computational Design of Metal-Free Catalysts for Catalytic Hydrogenation of Imines

Lili Zhao, Haixia Li, Gang Lu, Zhi-Xiang Wang*

SI1 Calibrations of the basis-set-size effect on the energetics

Table S1 Comparisons of the activation barriers (ΔE^\ddagger in kcal/mol) and the relative energies (ΔE in kcal/mol) of the product at the various computational levels, using the gas phase hydrogen activation ($\mathbf{5} + \text{H}_2 \rightarrow \mathbf{5}\text{-H}_2$) as an example.

Computational levels	ΔE^\ddagger^a	ΔE^a
M05-2X/6-31G(d,p)	14.9 ^b	4.5 ^b
M05-2X/6-311++G(d,p)	16.6 ^c	5.3 ^c
M05-2X/6-311++G(2d,p)/M05-2X/6-31G(d,p)	17.0 ^b	5.6 ^b
M05-2x/6-311++G(2d,p)//M05-2X/6-311++G(d,p)	17.1 ^c	5.6 ^c
M05-2X/6-311++G(3df,2p)//M05-2X/6-31G(d,p)	17.0 ^b	5.6 ^b
M05-2X/6-311++G(3df,2p)//M05-2X/6-311++G(d,p)	17.6 ^c	5.6 ^c
MP2/6-31G(d,p)	13.6 ^b	2.4 ^b
MP2/6-311++G(2d,p)//MP2/6-31G(d,p)	12.5 ^b	1.8 ^b

^a Relative to $\mathbf{5} + \text{H}_2$. ^b Corrected by M05-2X/6-31G(d,p) + ZPE. ^c Corrected by M05-2X/6-311++G(d,p) + ZPE.

SI2 Energetic and geometric results for **5** passing criteria I-III and the H₂ activation of **5**

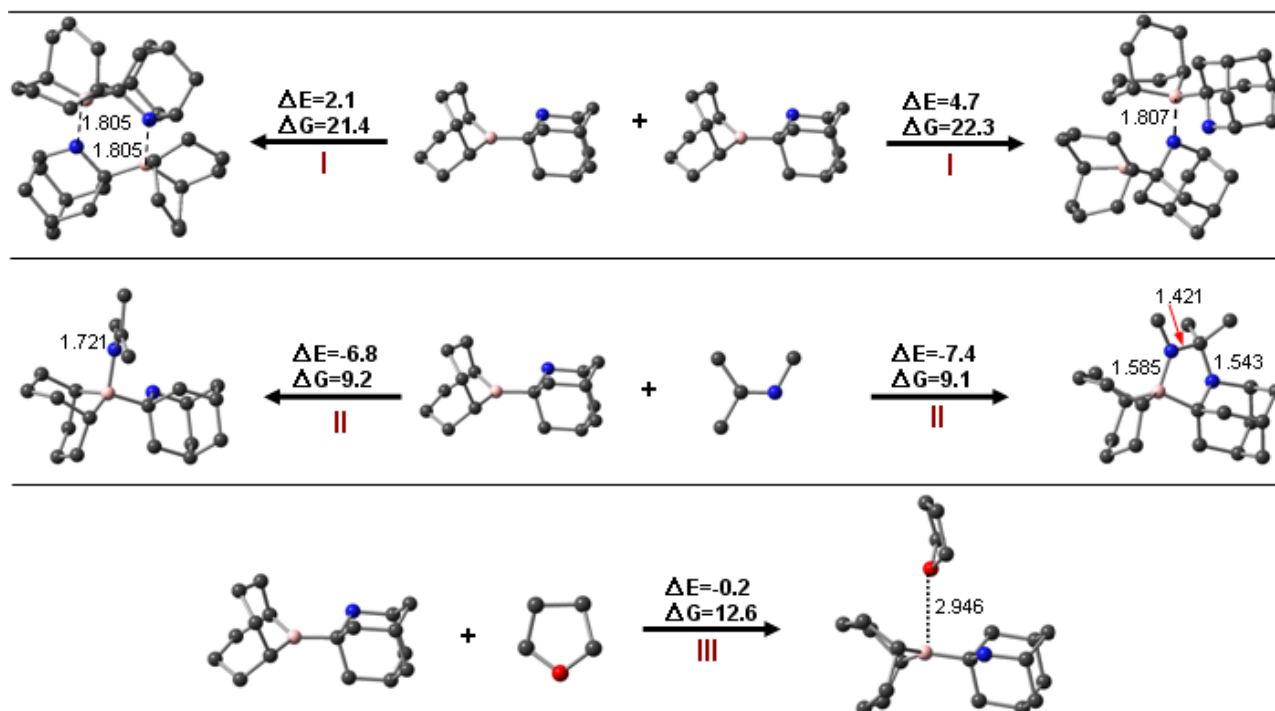


Fig. S2-1 Optimized structures and relative energies (in kcal/mol) of the complexes of **5** with **1** (imine) and THF (passing criteria I-III) at M0-52X/6-311++G(2d,p)//M0-52X/6-31G(d,p) + ZPE level, including the BSSE corrections.

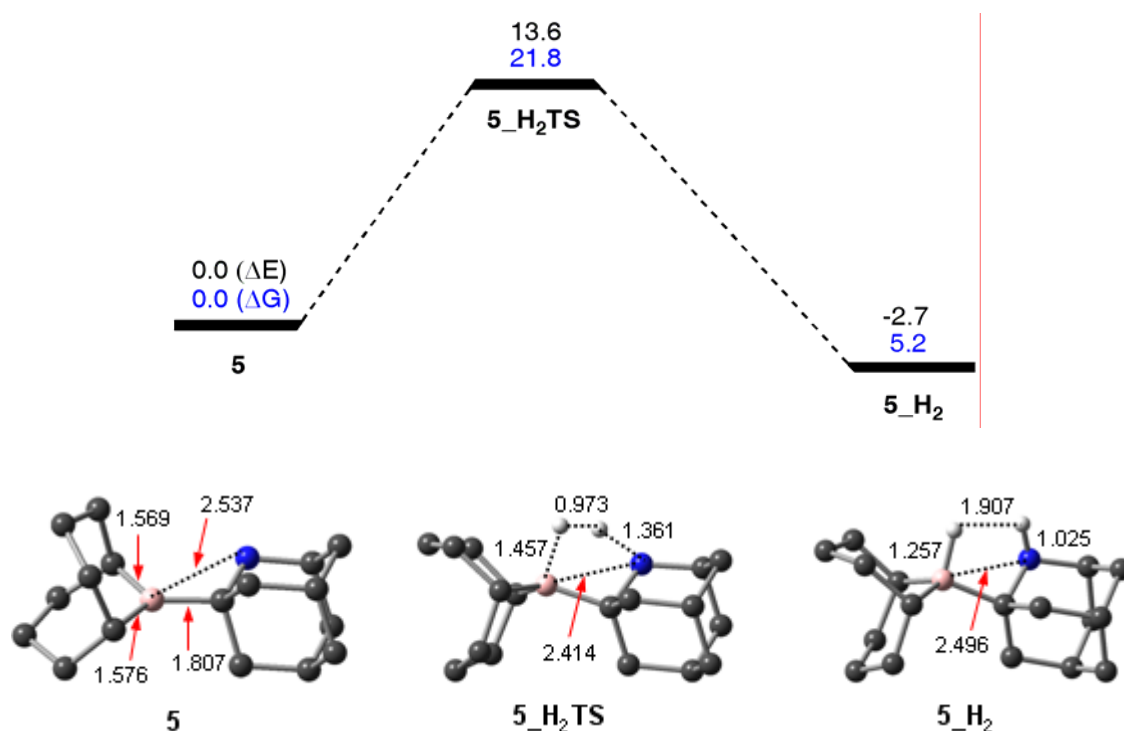


Fig. S2-2 Energy profile (in kcal/mol) and the optimized geometries for the H₂ activation step of **5** at M0-52X/6-311++G(2d,p)//M0-52X/6-31G(d,p) + ZPE level. The selected atomic distances are given in Å. Trivial hydrogen atoms are omitted for clarity.

SI3 Energetic and geometric results for the conformational change between **7** and **6** and their H₂ activations

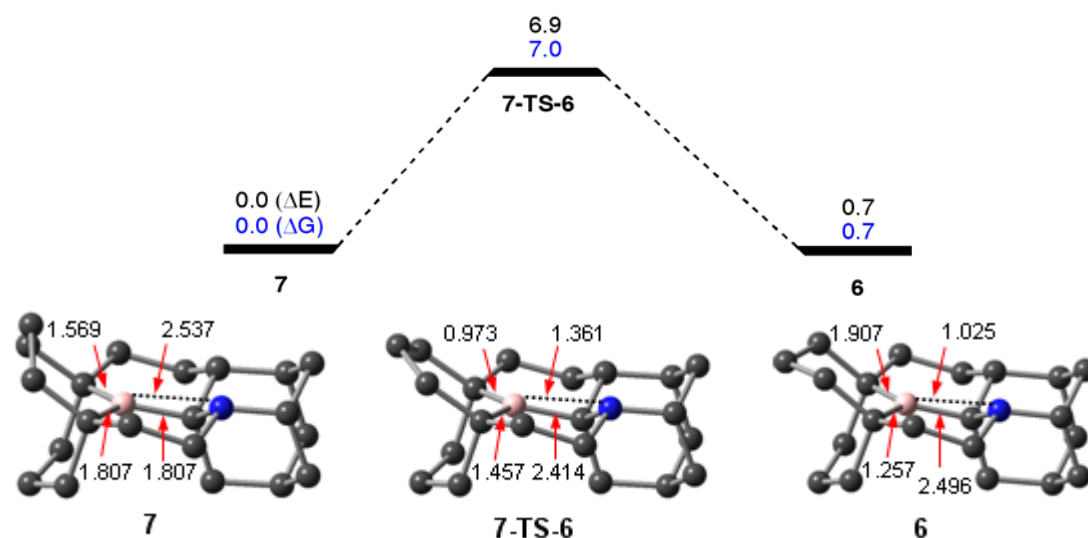


Fig. S3-1 Energy profile and the optimized geometries for conformational change between **7** and **6** at M05-2X/6-311++G(2d,p)//M0-52X/6-31G(d,p) + ZPE level. The selected atomic distances are given in Å. Trivial hydrogen atoms are omitted for clarity.

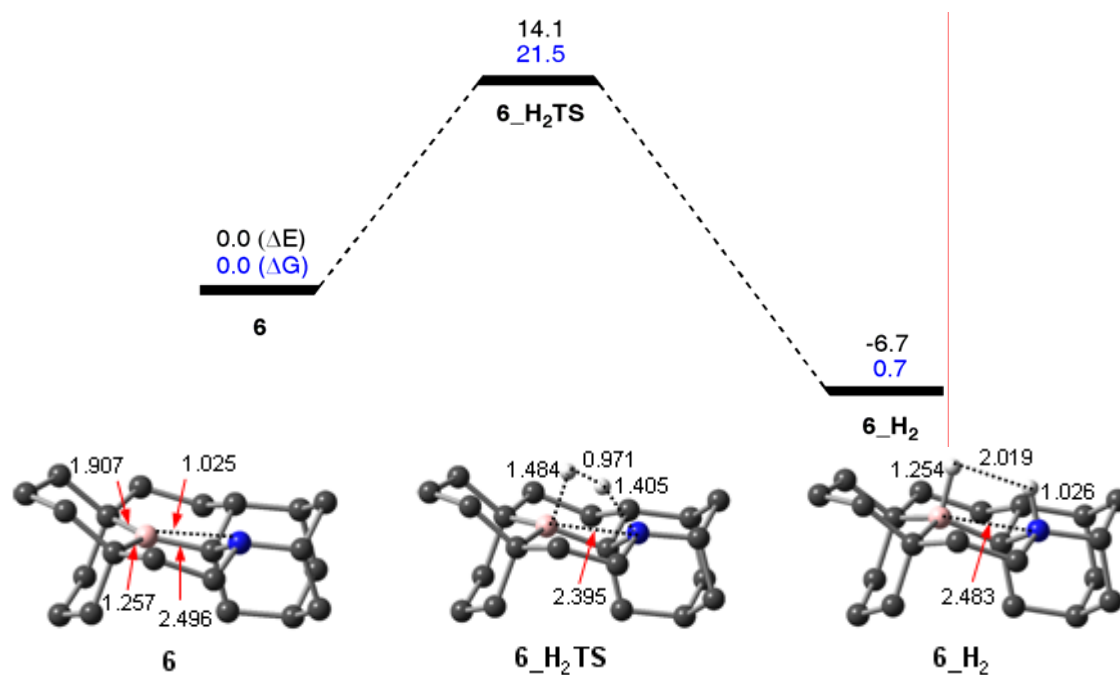


Fig. S3-2 Energy profile and the optimized geometries for the H₂ activation step of **6** at M0-52X/6-311++G(2d,p)//M0-52X/6-31G(d,p) + ZPE level. The selected atomic distances are given in Å. Trivial hydrogen atoms are omitted for clarity.

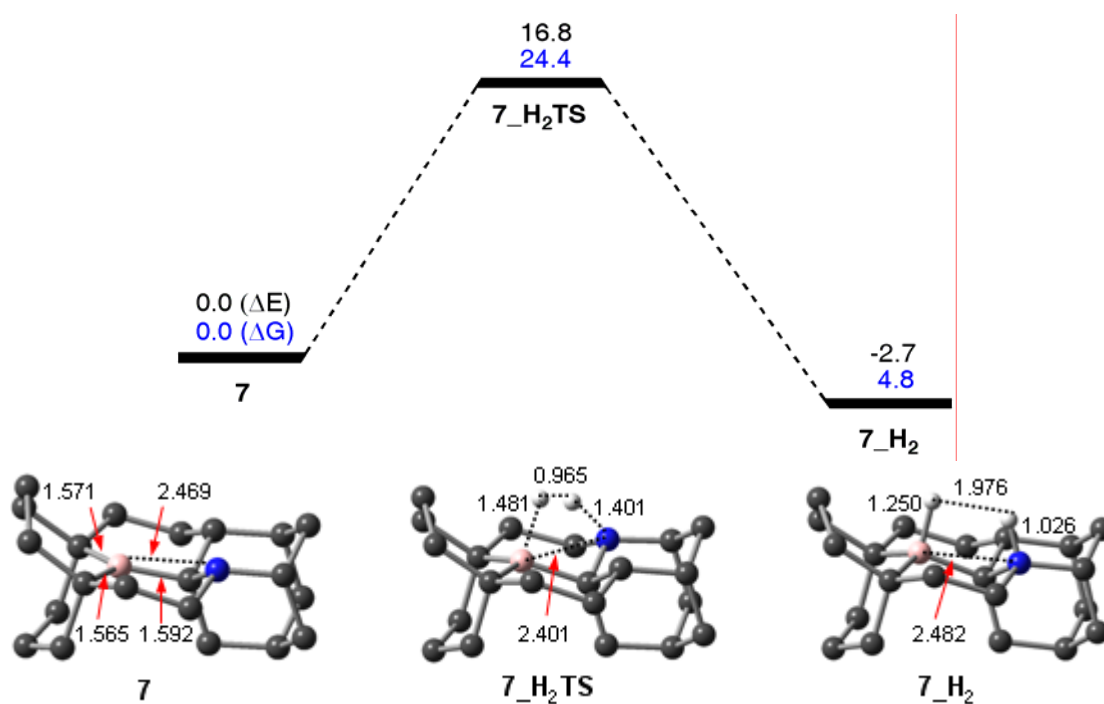


Fig. S3-3 Energy profile and the optimized geometries for the H₂ activation of **7** at M0-52X/6-311++G(2d,p)//M0-52X/6-31G(d,p) + ZPE level. The selected atomic distances are given in Å. Trivial hydrogen atoms are omitted for clarity.

SI4 Energetic and geometric results to verifying that **8** and **9** are able to pass Criteria I-III, and V

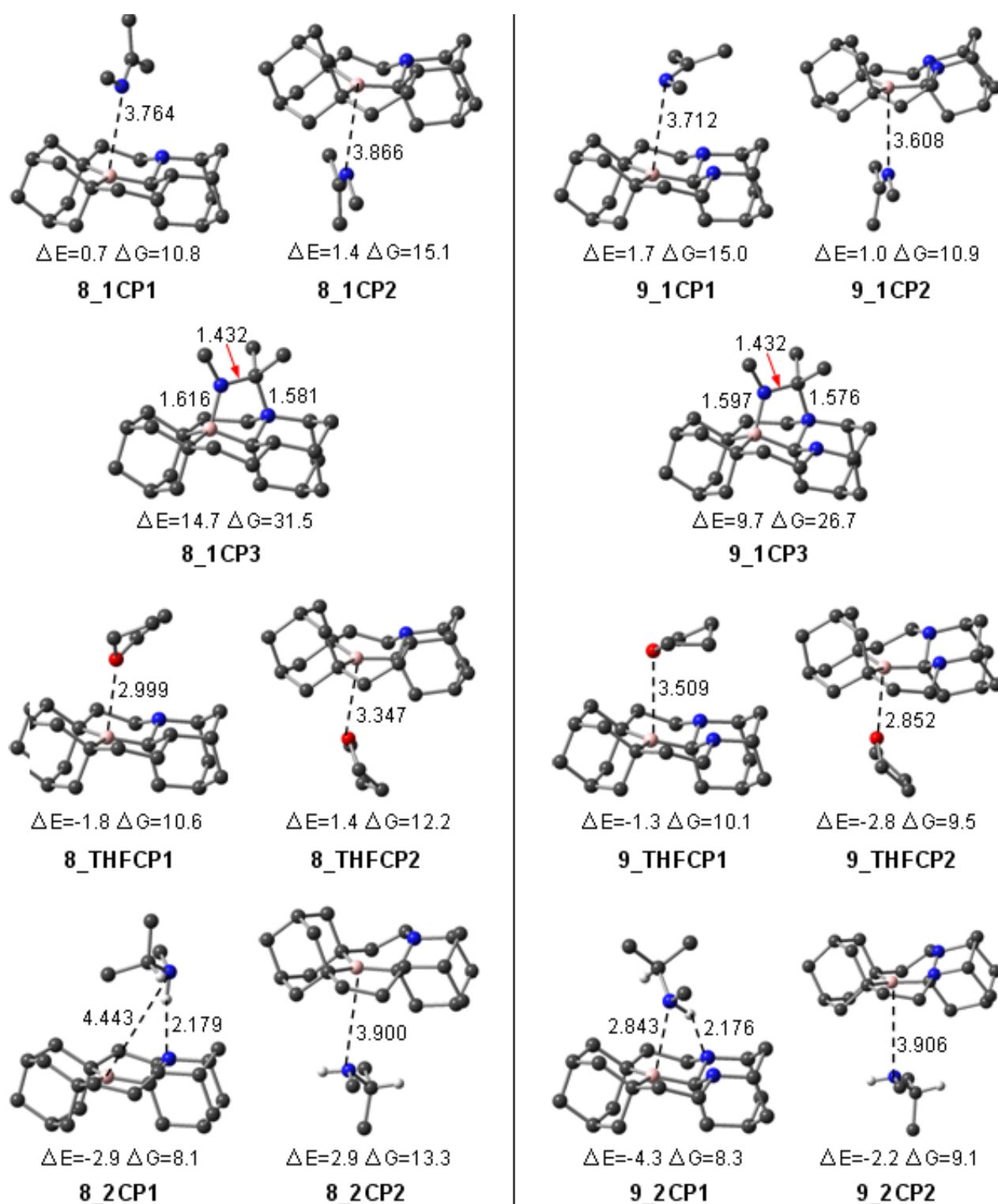


Fig. S4-1 M05-2X/6-31G(d,p) optimized structures of the complexes of **8** and **9** with **1**, **2** and THF. The ΔE and ΔG values are the binding energies and free Gibbs free energies (in kcal/mol) at the M05-2X/6-311++G(2d,p)(IEFPCM)/M05-2X/6-31G(d,p) + ZPE + BSSE level.

The built-in geometries of **8** and **9** can exclude the formation of intramolecular Lewis adducts like those drawn in Scheme 2. With regard to intermolecular dimerizations, we considered the dimerization of **5**, rather than those of **8** and **9** directly. **Fig. S4-2** shows the two types of dimers of **5**. The long B-N distances and the positive dimerization energies (2.1 and 4.7 kcal mol⁻¹, respectively, including BSSE corrections) indicate that **5** can not form stable dimer. **8** and **9** are apparently sterically more demanding than **5**, we thus concluded that they can not form stable dimers, passing Criterion I of Scheme 2.

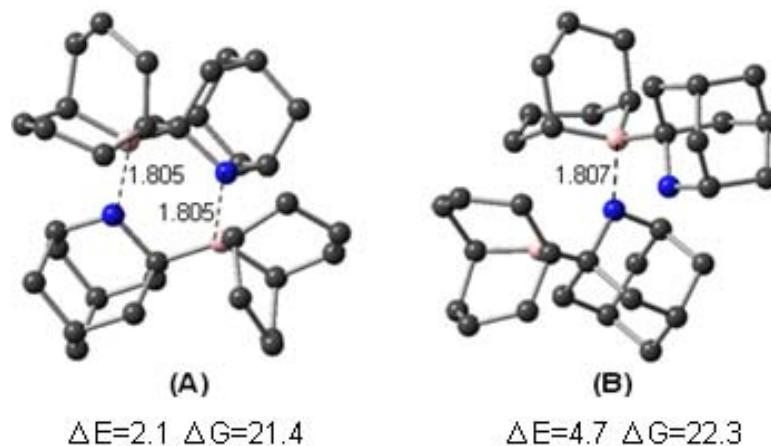


Fig. S4-2 M05-2X/6-31G(d,p) optimized dimers of **5**. (A) the dimer with two B-N dative bonds and (B) the dimer with one B-N dative bond.

SI5 Energetic and geometric results for the hydrogen activation of 2' and tBu₂PB(C₆F₅)₂

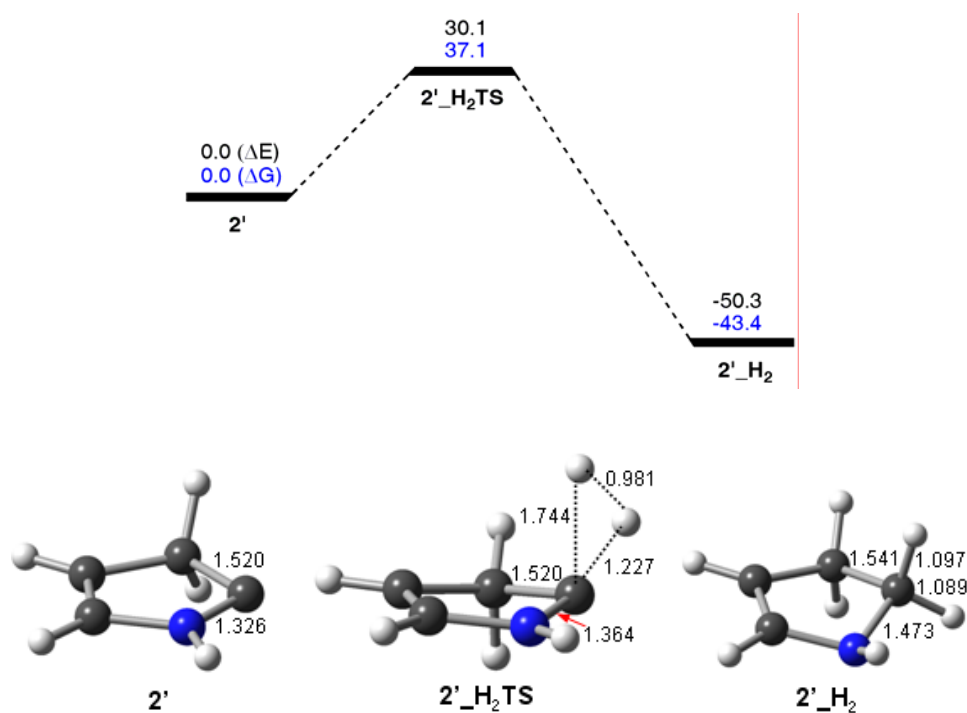


Fig. S5-1 Energy profile and the optimized geometries for the H₂ activation of 2' at M0-52X/6-311++G(2d,p)//M0-52X/6-31G(d,p) + ZPE level. The selected atomic distances are given in Å. Trivial hydrogen atoms are omitted for clarity.

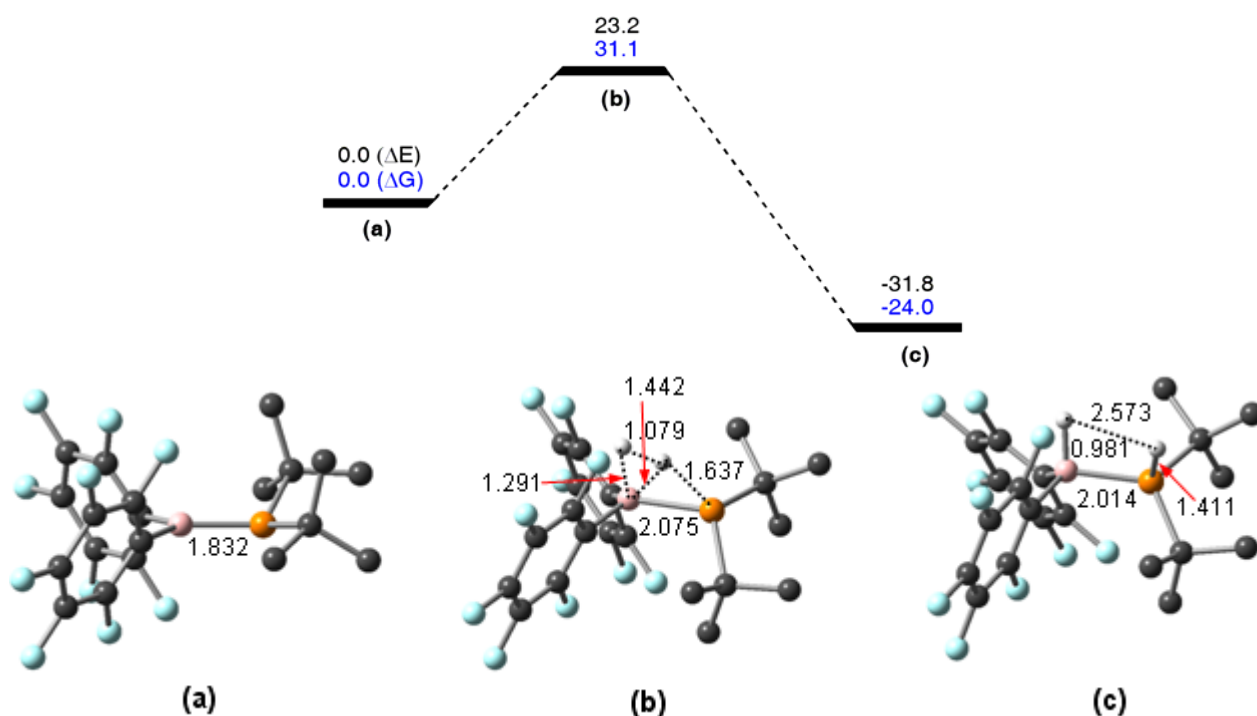


Fig. S5-2 Energy profile and the optimized geometries for the H₂ activation of tBu₂P-B(C₆F₅)₂ at M0-52X/6-311++G(2d,p)//M0-52X/6-31G(d,p) + ZPE level: (a) tBu₂PB(C₆F₅)₂, (b) tBu₂PB(C₆F₅)₂-H₂TS, (c) tBu₂PH-BH(C₆F₅)₂.

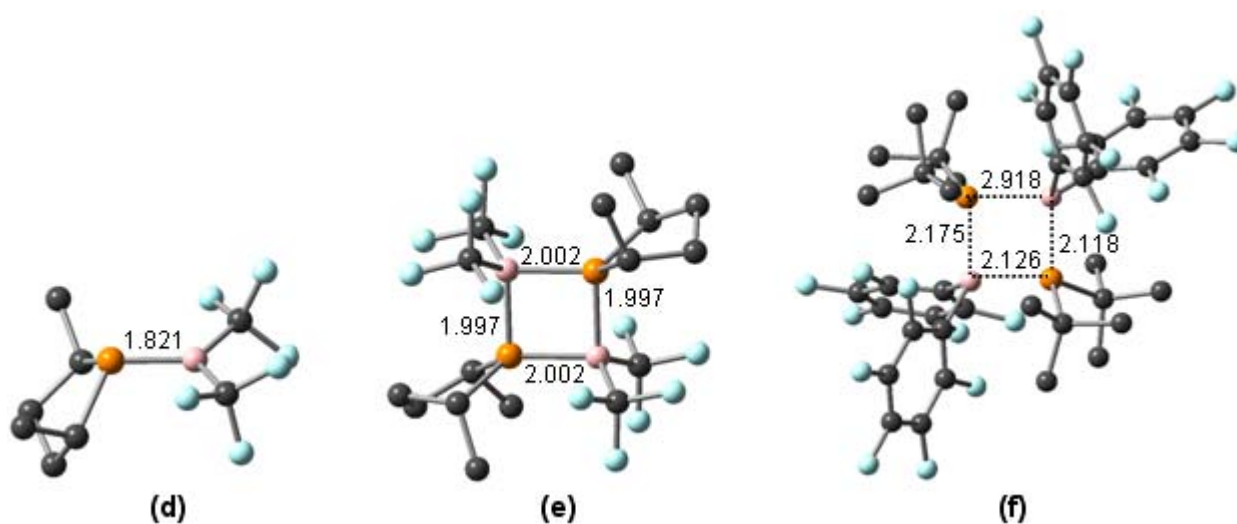


Fig. S5-3 Optimized structures of dimers of $(\text{CF}_3)_2\text{BPMe}_2$ and $\text{tBu}_2\text{PB}(\text{C}_6\text{F}_5)_2$ at M0-52X/6-31G(d,p) + ZPE level: (d) $(\text{CF}_3)_2\text{BPMe}_2$, (e) the dimer of $(\text{CF}_3)_2\text{BPMe}_2$, (f) the dimer of $\text{tBu}_2\text{PB}(\text{C}_6\text{F}_5)_2$.

SI6 Energetic and geometric results for the **8**-catalyzed hydrogenation

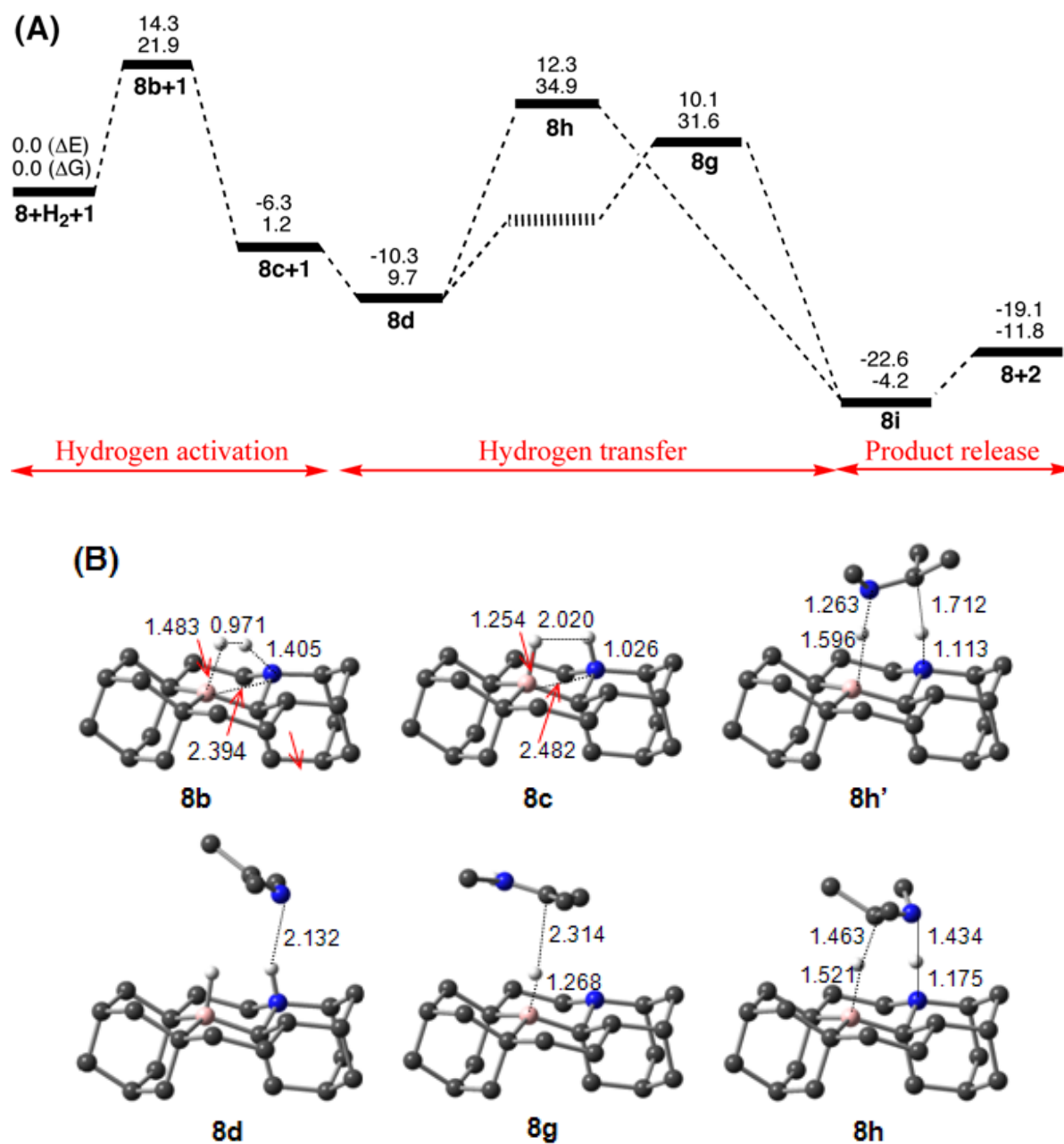


Fig. S6 (A) Energy profile for the reaction of H₂ + **8** + **1** in THF. (B) Optimized structures of the stationary points, along with the key bond distances in Å. Trivial hydrogen atoms are omitted for clarity.

SI7 The PES and the structures from **9d** to the protonated **1** (NHMe-CMe₂⁺) + **9**_BH⁻

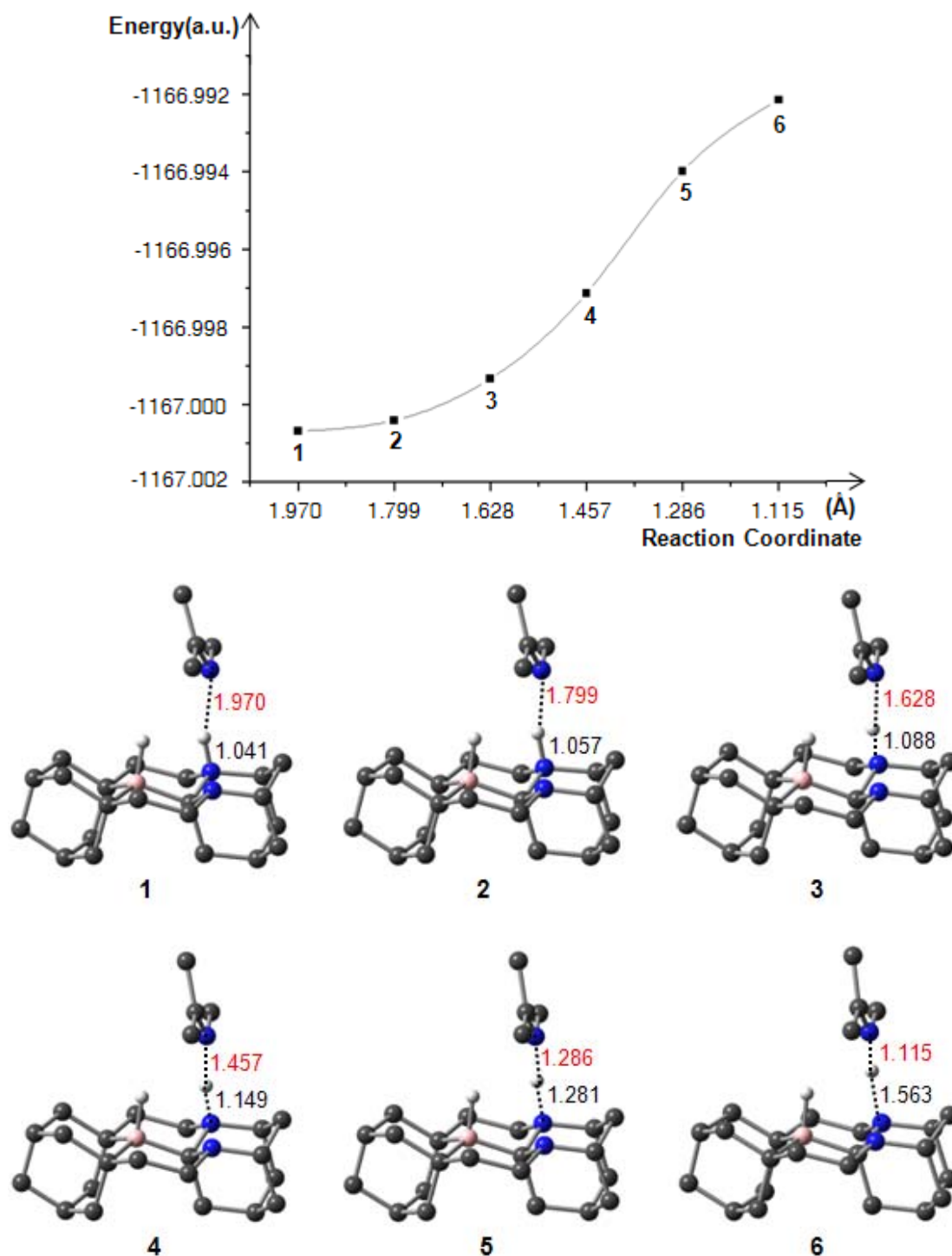


Fig. S7 Scanned potential energy surface (PES) from **9d** to the protonated **1** (NHMe-CMe₂⁺) + **9**_BH⁻ and the optimized structures of the points labelled on the PES at M0-52X/6-31G(d,p) level. The selected atomic distances are given in Å. Trivial hydrogen atoms are omitted for clarity.

SI8 Energetic and geometric results for the **11**-catalyzed hydrogenation

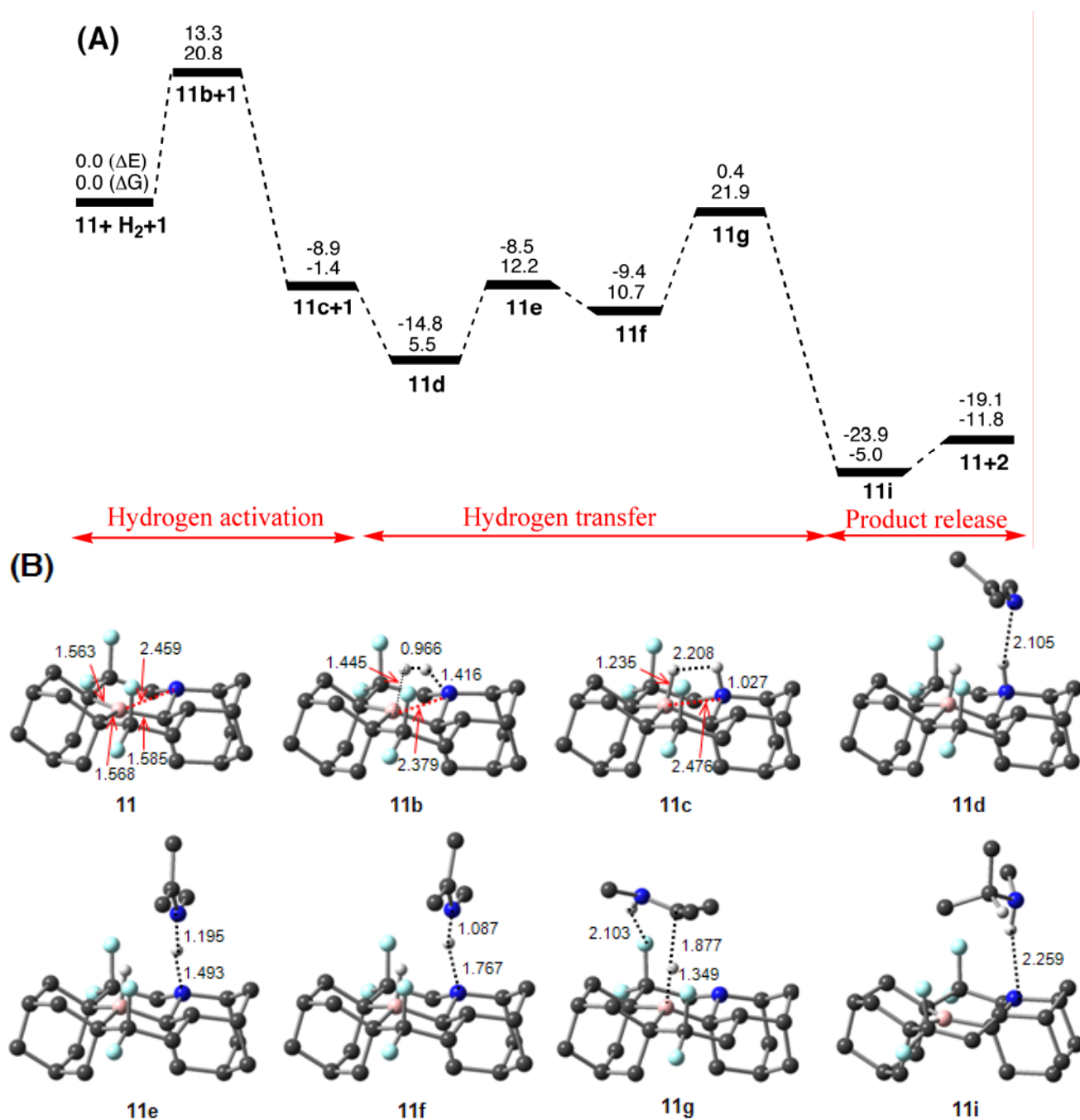


Fig. S8 (A) Energy profile for the reaction of $H_2 + \mathbf{11} + \mathbf{1}$ in THF. (B) Optimized structures of the stationary points, along with the key bond distances in Å. Trivial hydrogen atoms are omitted for clarity.

SI9 Optimized transition states involved in the three-component hydrogen activations of **8** and **11**

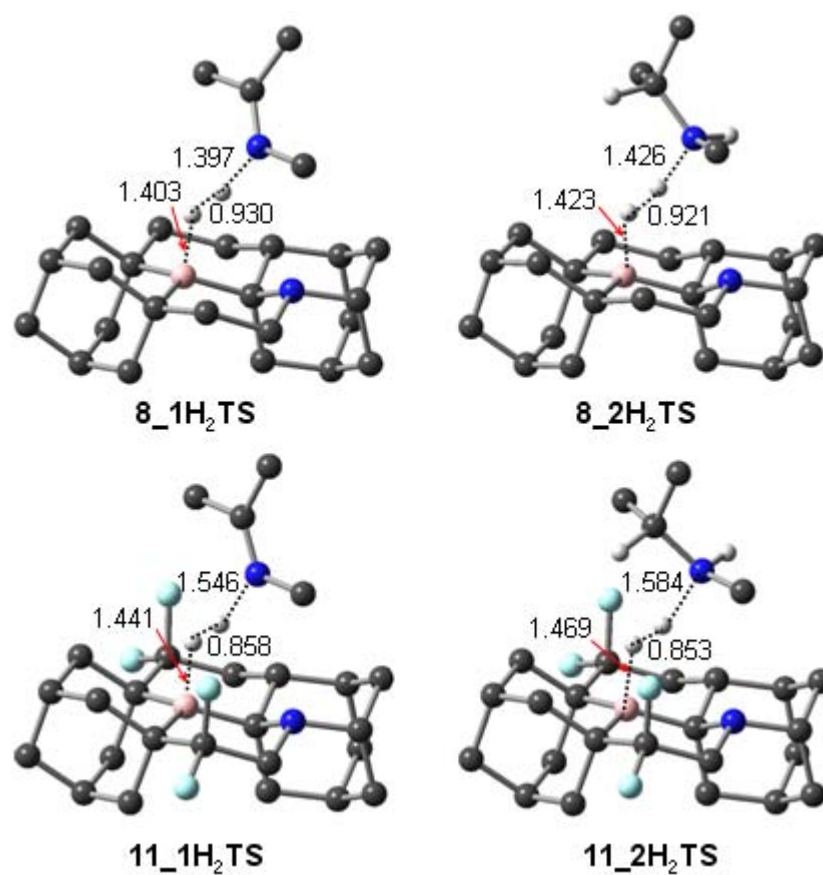


Fig. S9 Optimized structures of transition states for the three-component hydrogen activations reactions of **8** and **11** at M05-2X/6-31G(d,p) level, along with the key bond lengths in Å. Trivial hydrogen atoms are omitted for clarity.